Adsorption of Isolated, Flexible Polymers onto a Strongly Attracting Surface

A. L. Ponomarev

Department of Applied Physics and Applied Mathematics, Columbia University, New York, New York 10027

T. D. Sewell

Los Alamos National Laboratory, Theoretical Division Los Alamos, New Mexico 87545

C. J. Durning*

Department of Chemical Engineering and Applied Chemistry, Columbia University, New York, New York 10027

Received June 2, 1998

ABSTRACT: We investigate by lattice Monte Carlo simulation the kinetics of adsorption of isolated linear homopolymers onto a flat surface with a strong, short-ranged attraction for the segments. We focus on limiting cases corresponding to strong physisorption and chemisorption. Initially, the polymer has a conformation representative of the bulk (dilute) solution, but with a few peripheral segments in contact with the surface. Subsequent adsorption is tracked by monitoring a number of mechanical variables. By averaging over initial configurations, and over appropriately selected time windows along individual trajectories, we determine the adsorption kinetics and find the effects of chain length and segment/surface interactions on the characteristic time for adsorption, τ_{ads}. For all situations investigated, τ_{ads} increases algebraically with the number of segments N; i.e., $\tau_{ads} \sim N^{\alpha}$, with α being considerably *smaller* than that for scaling of the bulk relaxation time of the chain, τ_R. We find that α depends on the details of the short-ranged surface/segment interaction potential. The results are rationalized with scaling-level analysis.

I. Introduction

The adsorption of flexible polymers at interfaces is of great technological interest[1,2] primarily because it can *significantly* and *permanently* modify the interfacial properties. The most dramatic and stable modifications result from high-density layers of chains bound strongly at the interface. The common approaches to achieve such layers exploit either strong physisorption of segments or covalent "grafting" of chains, i.e., chemisorption.[3,4] Strong physisorption involves favorable, noncovalent, local interactions with energies exceeding kT (e.g., permanent dipole or electrostatic interactions) between at least some groups on the adsorbing polymer and interfacial sites. Chemisorption or grafting of chains involves chemical reaction between groups on the polymer and interfacial sites, which creates permanent attachments to the interface by covalent bonds. For both strong physisorption and chemisorption, it is often inappropriate to assume thermal equilibrium when considering the structure of the adsorbed layer[5−8] since the adsorbing polymers get trapped in long-lived, or permanent, nonequilibrium states. There is considerable practical value in studying the nonequilibrium features of such systems to determine what, if any, universal characteristics emerge, and how these can be manipulated through the polymer/surface chemistry or the contacting conditions between the polymer and the surface. Toward this end, we investigate by lattice Monte Carlo simulations the adsorption kinetics of isolated, linear polymers adsorbing onto a smooth, flat, strongly attractive surface, the specific goal being a clear understanding of the transient process.

* Corresponding author.

The adsorption of isolated chains is one of the simplest nonequilibrium processes involving polymers at an interface, yet only a few studies of this scenario exist for strongly attractive surfaces.[7,9] Although quite a few applications involve many interacting chains at interfaces, the adsorption of isolated chains is directly relevant to a number of emerging single-molecule approaches to molecular genomics.[10,11] In addition, a thorough study of isolated chains provides a valuable benchmark for studies of many-chain systems.

Our lattice simulations are specifically designed to mimic strong physisorption and chemisorption. In order to mimic strong physisorption, we consider that adsorption of a segment has no local activation barrier and involves a relatively deep energetic well at the interface. At the same time, lateral stochastic motion of segments on the surface is permitted. For chemisorption, segment adsorption involves a significant local activation barrier. The computational approach is based on the bond fluctuation (BF) algorithm invented by Carmesin and Kremer.[12] This lattice algorithm accurately reproduces universal static and dynamic scaling for phantom and self-interacting polymers in bulk, for both dimensions $D = 2$ or $D = 3$.[12−14] Consequently, it offers a promising tool for dynamic simulation of adsorption. Indeed, several previous workers have exploited BF to study polymers interacting with surfaces.

Lai[15,16] studied equilibrium statics and dynamics of physisorbed, self-avoiding polymers as a function of chain length, N, and the energy of segment−surface interactions, ϵ_s, which defines a dimensionless surface "temperature", $T_s \equiv kT/\epsilon_s$. He showed[15] that BF correctly captures the critical scaling of the well-known adsorption transition for linear self-avoiding walks on attrac-

10.1021/ma9808732 CCC: $19.00
Published on Web 03/09/2000

tive surfaces.[17] For T_s below the transition temperature, he found that the in-plane diffusion coefficient $D_{||}$ obeys Rouse scaling, while, at the same time, the perpendicular component $D_{\perp}$ drops to zero.

In another prior effort, Shaffer[18] used BF to study physisorption kinetics of linear, self-avoiding homopolymers and copolymers (where only a fraction of the segments adsorb). For homopolymers, he found that the characteristic time of adsorption, τ_{ads}, obeyed $\tau_{ads} \sim N^{\alpha}$, where $\alpha = 1.58 \pm 0.04$, a law that has not yet been explained from a fundamental point of view. These works reinforce that BF provides a reliable tool for studying dynamics of polymers interacting with surfaces.

In the next section, we summarize our model for an attractive interface and the simulation methods. Two different regimes of behavior are anticipated, depending on whether segmental adsorption is rapid or slow compared to the chain's bulk relaxation time, τ_R; these are identified loosely with strong physisorption and chemisorption, respectively. Following that, we discuss simulation results for the two cases; very different mechanistic features emerge for each. Exponents α for the N-scaling of the characteristic time for adsorption τ_{ads} differ dramatically in the two cases, and for both lie considerably below the exponent for τ_R. The final section of the paper rationalizes the α found using a scaling analysis.

II. Computational Details

A. Bond Fluctuation Algorithm. We utilized a lattice model that represents the polymer segments or monomers as a sequence of occupied sites on a lattice. Brownian motion is simulated by iterative, local displacement of segments using the Metropolis method:[19] On each machine iteration, a segment is chosen at random and displaced to a neighboring site by random selection of a move from an allowable set that crudely mimics thermally stimulated segmental motions possible in real chains. By biasing the acceptance of each move using the principle of detailed balance, one generates a sequence of states that approaches and eventually realizes the equilibrium distribution, i.e., the chain's canonical ensemble distribution (see ref 20 for a detailed discussion). It has been shown that the Markov chain of states generated by such lattice models faithfully mimics the long-wavelength real-time dynamics of polymers in bulk regardless of the details of local segmental moves.[21,22]

The particular lattice algorithm we used was bond fluctuation (BF) invented by Kremer and co-workers.[12] When carried out on a 3-D cubic (2-D square) lattice, the allowed segmental moves are simple lateral jumps to one of six (four) nearest-neighbor sites. The algorithm permits fluctuation in the distance between adjacent monomers, i.e., in the length of backbone "bonds". The minimum bond length allowed (two units on a square or cubic lattice) prevents overlap of adjacent segments in the chain, while the maximum length ($\sqrt{13}$ or $\sqrt{10}$ units on a square or cubic lattice, respectively) ensures that backbone bonds cannot cut one another in a self-avoiding chain. An important advantage of this algorithm is that it appears to remain ergodic up to relatively high densities, and in low dimension, making it valuable for situations involving interfaces.

We simulated both phantom, random walk chains (RWs) and self-avoiding noncrossable chains (SAWs). The chain is confined in a $\simeq 2N \times 2N \times N$ cell with a commensurate square lattice along the broad side interacting with segments via a strong, short-ranged potential (see below). During adsorption the chain's center of mass never drifts away from the adsorbing plane and is periodically realigned with its center so that segments never encounter the cell's free boundaries. (Of course, the displacements needed to realign are recorded to track the in-plane center of mass motion.) This procedure corresponds to infinite dilution conditions. There is an algorithmic complication because two distinct sets of allowable bond lengths are required for cubic and square lattices.[12,13] We used 2-D rules for segments in trains and 3-D rules for segments in loops and tails together with an explicit check to prevent bond cutting on the surface or in the bulk by segmental moves to or from the surface, respectively (see ref 23 for more details).

B. Interface Potential and Surface Friction. Let z be the distance normal to the adsorbing surface in units of the lattice spacing. To include that segments may have to surmount a local activation barrier of height ϵ_b in order to access the surface, moves from $z = 2$ to $z = 1$ are biased by a probability $p_b = \min\{1, \exp -1/T_b\}$, $T_b \equiv kT/\epsilon_b$, while leaving unbiased moves from $z = 1$ to $z = 2$. The simulation includes that when a segment contacts the surface it loses an energy ϵ_s by biasing moves from $z = 0$ to $z = 1$ by the probability $p_s = \min\{1, \exp -(1/T_s + 1/T_b)\}$, while leaving unbiased moves from $z = 1$ to $z = 0$. Once a segment lies on the surface, it can jump to neighboring surface sites to simulate the effects of surface diffusion. By biasing the probability of *all* such moves with $p_{xy} = \min\{1, \exp -\epsilon_{xy}/kT\}$, one retards the intrinsic hopping frequency of segments on the interface relative to that in the bulk; here ϵ_{xy} corresponds to a local barrier between adjacent sites on the surface. In terms of segmental friction factors[22] for the bulk and on the surface, ζ_b and ζ_s, respectively, applying $p_{xy} \leq 1$ corresponds to the ratio $\zeta_s/\zeta_b = \exp \epsilon_{xy}/kT \geq 1$.

These biasing procedures enforce the detailed balance requirements for transition probabilities between neighboring states that ensure the correct distribution of configurations at equilibrium.[20] The interfacial conditions of a particular simulation are specified by the four parameters N, T_s, T_b, and ζ_s/ζ_b.

C. Initial States. For each realization, the initial configuration is representative of an isolated chain in 3-D bulk, but with a few peripheral segments touching the wall. This was accomplished in a three-step procedure. First a bulk configuration was generated by a standard SAW algorithm,[24] with the length of each bond fixed at two lattice spacings. Second, since the SAW generated in the first step does not reproduce the equilibrium distribution of bond lengths and angles in a BF calculation, 3-D bulk BF "dynamics" were run for times longer than the chain's longest relaxation time, τ_R. Finally, the equilibrated, bulk configuration was translated in the $-z$ direction until the first monomer/surface contact(s) occurred.

D. Averaging. After an initial state is established, the hybrid 2-D/3-D BF dynamics described earlier are used to generate a realization, during which the chain adsorbs onto the surface and eventually settles into a fluctuating equilibrium state. For each realization, we continued the Markov chain until the perpendicular component of the center-of-mass position achieved a

steady-fluctuating value; the number of Monte Carlo steps (MCS) needed depends on N, T_s, T_b, and ζ_s/ζ_b and fell in the range $(1.5-5.0) \times 10^4$ MCS for our calculations. (N machine iterations, resulting on average in one attempted move per segment, corresponds to a fixed increment of physical time and is denoted as a Monte Carlo step (MCS).) We determined the evolution of various quantities (see next section) by averaging their values over a large number M of initial states; typically, $M \sim O(10^2)$ was feasible. This gave reasonably low uncertainties in the measured parameters. To further reduce uncertainties, we also averaged over appropriately selected time windows, Δt, along individual trajectories: typically $\Delta t \sim O(10^3$ MCS). In what follows, we denote averaged quantities with brackets $\langle ... \rangle$.

E. Quantities Measured. During each realization, we measured four parameters characterizing the overall location, size, and shape of the chain: the z component of the chain's center-of-mass position, $\mathbf{R}_{com}$

$$\mathbf{R}_{com} = \frac{1}{N}\sum_{i=1}^{N}\langle \mathbf{R}_i \rangle \tag{1}$$

where $\mathbf{R}_i$ means the position of segment i, and the in-plane and perpendicular contributions to the radius of gyration, $R_{g,||}$ and $R_{g,\perp}$, respectively

$$R_{||}^2 = \left\langle \frac{1}{N}\sum_{i=1}^{N}[(R_{i,x} - R_{com,x})^2 + (R_{i,y} - R_{com,y})^2] \right\rangle, \tag{2}$$

$$R_{\perp}^2 = \left\langle \frac{1}{N}\sum_{i=1}^{N}(R_{i,z} - R_{com,z})^2 \right\rangle \tag{3}$$

$$R_g^2 = R_{\perp}^2 + R_{||}^2 \tag{4}$$

Another key parameter characterizing the overall progress of adsorption is the fraction of adsorbed monomers $\chi(t)$. Since the equilibrium value $\lim_{t\to\infty}\langle\chi(t)\rangle \equiv \chi_{eq}$ depends on T_s,[15] a normalized function $q(t)$ proves convenient

$$q(t) = \frac{\chi_{eq} - \langle\chi(t)\rangle}{\chi_{eq} - \langle\chi(0)\rangle} \tag{5}$$

We also determined several parameters that reveal mechanistic details of the adsorption process. A mechanism in one limiting case is "zipping" onto the surface, which occurs exclusively by the consecutive, sequential adsorption of segments, as illustrated in Figure 1. A measure of the extent of zipping is the cumulative fraction of sequential monomer adsorptions, with one or both neighboring segments already adsorbed, $p^{seq}(t)$. This tends toward unity when zipping dominates but has lower values otherwise. As a benchmark, one can find for $T_s = 0$ and no spatial correlations among monomers, i.e., considering random adsorption of unconnected particles, $\lim_{t\to\infty;N\to\infty} p^{seq}(t) = 2/3$ (Appendix A). A transient structural feature depending sensitively on the zipping effect is the loop distribution. If zipping dominates during adsorption, relatively few loops will be formed. Consequently, we determined the average number of loops at time t, $L^{tot}(t)$, and the average number of monomers per loop, $N^{loop}(t)$.

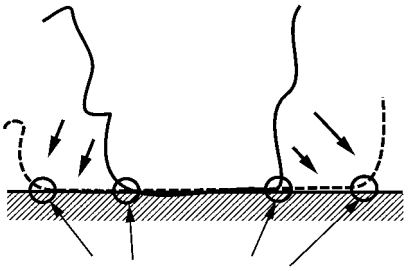

Figure 1. Schematic of a zipping process expected for a deep surface well and no local activation barrier ($T_s \to 0$; $T_b \to \infty$), implying that the characteristic ratio $\tau_b/\tau_R \ll 1$ (see eq 8). The chain adsorbs by the sequential, consecutive attachment of segments onto the surface. During the entire process, the number of contact points, i.e., of loops, remains $\sim O(1)$.

Table 1. Scaling Exponents for *N*-Dependence of Bulk Properties for SAWs

D	R_g^2		τ_R
2		-1.0 ± 0.1	2.4 ± 0.3
3	1.21 ± 0.05	-1.06 ± 0.03	2.3 ± 0.4

F. Characteristic Times. We determined characteristic times for adsorption, τ_{ads}, from the rate of monomer adsorption using the relaxation function $q(t)$ (see eq 5). It turned out that $q(t)$ decays exponentially during most of the adsorption process; deviations are seen only at very short and very long times. Thus, τ_{ads} was found from regression fits of

$$q(t) = c \exp\frac{-t}{\tau_{ads}} \tag{6}$$

to the linear portion of $q(t)$ vs t data.

Note that τ_{ads} reflects only the rate of monomer precipitation onto the surface. To check whether this provides a unique characteristic time for the adsorption process, we compared τ_{ads} with the time scales associated with the evolution of $R_{g\perp}$, $R_{g||}$, and the z-component of $\mathbf{R}_{com}$, denoted $\tau_\perp$, $\tau_{||}$, and τ_{com}, respectively.

III. Results

A. Benchmarks. We first checked that our BF code gave the correct bulk static and dynamic scaling for isolated chains in D = 2 and D = 3. The Flory exponent ν_D was determined from log−log plots of $\langle R_g^2\rangle$ vs N, for $10 \le N \le 180$, averaging over $M \sim O(10^2)$ and $\Delta t \sim O(10^4$ MCS); recall $R_g \sim N^{\nu_D}$ where $\nu_3 \simeq 0.59$ and $\nu_2 \simeq 0.75$.[21,22] The N scaling of center-of-mass diffusion coefficients D and autocorrelation times τ_R was also obtained, from the long-time slope of $\langle[\mathbf{R}_{com}(t) - \mathbf{R}_{com}(0)]^2\rangle$ vs t and its intersection with $\langle[\mathbf{R}_{com}(t) - \mathbf{R}_{com}(0)]^2\rangle = {}^2/_3 R_g^2$, respectively, using roughly the same M and Δt; scaling predictions from the Rouse model are $D \sim N^{-1}$ and $\tau_R \sim N^{1+2\nu_D}$.[21,22] Table 1 summarizes our benchmark results; within uncertainty, all agree with expectations.

B. General Features. As mentioned earlier, our primary aim is to study situations mimicking strong physisorption and chemisorption. In both cases, T_s is small while ζ_s/ζ_b is of order one or exceeds unity; the former condition strongly suppresses desorption of monomers, while the latter retards their mobility on the surface. Thus, the key difference between strong physisorption and chemisorption in this coarse-grained picture is the values of T_b, characterizing the local

activation barrier for a segment to access the surface. For physisorption the barrier is low ($T_b > O(1)$), while for grafting it is high ($T_b < O(1)$).

Consider that T_b sets a characteristic time τ_b for the passage of a segment across the barrier, given that it already lies immediately adjacent to it

$$\tau_b \simeq \tau_o \exp \frac{1}{T_b}, \tag{7}$$

where τ_o is an intrinsic hopping time in the bulk. We found very different adsorption dynamics depending on the ratio of τ_b and the Rouse time τ_R:

$$\frac{\tau_b}{\tau_R} \simeq N^{-1-2\nu_3} \exp \frac{1}{T_b} \tag{8}$$

For $\tau_b/\tau_R \ll 1$, segments near the surface adsorb quickly, perturbing the chain out of its initial configuration. Here, the process can eventually drag the chain strongly out of equilibrium. Since N is always large, whenever $T_b \geq O(1)$, $\tau_b/\tau_R \ll 1$ and this scenario can arise. This corresponds qualitatively to strong physisorption.

On the other hand, for a fixed value of N, if the local barrier is high enough (T_b low enough) that $\tau_b/\tau_R \gg 1$, segments near the surface take a sufficiently long time to adsorb that the part of the chain extending into the bulk remains in pseudoequilibrium. Very different dynamics result in this case. Relatively short chains and small values of T_b lead to this regime, which corresponds most closely to chemisorption or grafting.

In the next section, we discuss results for situations resembling strong physisorption, meaning a deep surface well and no local activation barrier, so that $\tau_b/\tau_R \ll 1$. In order to obtain the fullest picture of this case with a minimum of computation, we fixed $T_s = 0$, $T_b \to \infty$ and varied the remaining parameters N and ζ_s/ζ_b over wide ranges (including $\zeta_s/\zeta_b \ll 1$, which does not correspond to a real physical situation). In the section following that, values of $T_b < 1$ are examined in an effort to mimic chemisorption.

C. Fast Adsorption ($\tau_b/\tau_R \ll 1$). Consider the behavior when there is no local barrier, in the case where $\tau_b/\tau_R \ll 1$, resembling strong physisorption. Recall that $q(t)$ tracks the fraction of unadsorbed monomers (eq 5). We found after an initial induction ln $q(t)$ falls nearly linearly with t for a significant portion of the process, indicating exponential decay (eq 6); τ_{ads} was obtained from the regression slope of the linear part of ln $q(t)$ vs t ($\tau_{ads} = -1/\text{slope}$).

Note that although τ_{ads} measures the time scale for adsorption, it does not necessarily give the time to reach equilibrium. For SAWs, equilibration involves (i) flattening, where the chain collapses against the surface onto its footprint, of size $R \simeq aN^{\nu_3}$, where a is the segment length, and (ii) spreading, where the chain expands laterally on the surface toward its equilibrium in-plane size, in the range $aN^{\nu_3} < R < aN^{\nu_2}$. Whenever $\tau_b/\tau_R \ll 1$, we found that the relative rates of flattening and spreading were about the same, except when ζ_s/ζ_b becomes quite large, at least of order 10^2 for $N = 100$.

The first important point from the simulations is that in this regime τ_{ads} appears to be a unique characteristic time for adsorption, i.e., for flattening of the chain against the surface. Figure 2 illustrates this point, by showing the evolution of $\langle R_\perp^2 \rangle$ and $\langle R_\parallel^2 \rangle$ against scaled time t/τ_{ads} for SAWs with $T_s = 0$, $T_b \to \infty$, $N = 100$, and several values of ζ_s/ζ_b. For $\zeta_s/\zeta_b = 1.0$ and 0.1, $\langle R_\perp^2 \rangle$ decays while $\langle R_\parallel^2 \rangle$ increases monotonically, the former corresponding to flattening and the latter to spreading; the data indicate no significant separation of time scales for the two processes, and that both $\langle R_\perp^2 \rangle$ and $\langle R_\parallel^2 \rangle$ relax on a scale $\sim\tau_{ads}$. Calculations for other values of N gave essentially the same results, indicating that the N-dependence of τ_{ads}, $\tau_\perp$, and $\tau_\parallel$ are the same for $\zeta_s/\zeta_b \lesssim 1$. It is only when ζ_s/ζ_b becomes quite large, $\gtrsim 10^2$ for $N = 100$ and $T_s = 0$ for example, that a discrepancy clearly emerges between the time scales for flattening and spreading. The case $\zeta_s/\zeta_b \to \infty$, where spreading is completely quenched, is included in Figure 2. Note that while $\langle R_\parallel^2 \rangle$ hardly changes, since the chain does not spread significantly, $\langle R_\perp^2 \rangle$ *still* relaxes on a scale $\sim\tau_{ads}$; i.e., τ_{ads} still characterizes flattening and adsorption of the chain. Further, the various measures of the characteristic time for flattening (τ_{ads}, $\tau_\perp$, and τ_{com}) were always of the same order and showed nearly identical scaling with N regardless of the surface friction (see subsequent discussion). We conclude that τ_{ads} is indeed a unique characteristic time for adsorption when $\tau_b/\tau_R \ll 1$ (eq 8), regardless of the relative surface friction, ζ_s/ζ_b, although it does not necessarily give the overall equilibration time. Before discussing results for τ_{ads} in more detail, consider evidence for a zipping mechanism when $\tau_b/\tau_R \ll 1$.

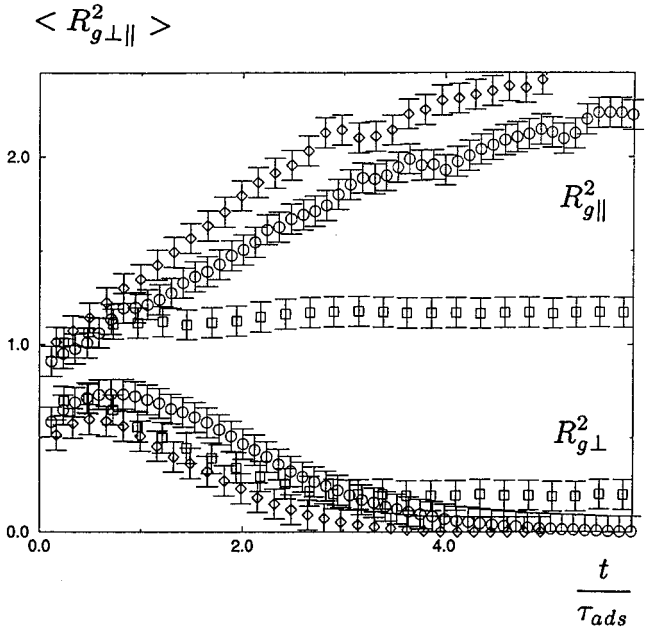

Figure 2. $\langle R_\perp^2 \rangle$ and $\langle R_\parallel^2 \rangle$ vs t/τ_{ads} for SAWs with $T_s = 0$, $T_b \to \infty$, $N = 100$, and several values of ζ_s/ζ_b: (○) $\zeta_s/\zeta_b = 1.0$; (◇) $\zeta_s/\zeta_b = 0.1$; (□) $\zeta_s/\zeta_b \to \infty$. For averaging, $M \simeq 100$ and $\Delta t = 5 \times 10^3$ MCS.

Figures 3−5 show representative results for the sequential adsorption probability, $p^{seq}(t)$, the average number of loops, $L^{tot}(t)$, and the average loop size, $N^{loop}(t)$, respectively. The calculations are for SAWs with $T_s = 0$, $\zeta_s/\zeta_b = 1.0$, and $N = 100$; consider for now just the results for $T_b \to \infty$ when $\tau_b/\tau_R \ll 1$ ((○) in Figures 3-5). Throughout adsorption, $p^{seq}(t)$ lies well above the benchmark of $^2/_3$ for randomly adsorbed particles (Appendix A), indicating a preponderance of monomer adsorptions with an adjacent monomer already attached (Figure 3). At the same time, $L^{tot}(t)$ (Figure 4) and $N^{loop}(t)$ (Figure 5) decay monotonically from the values established initially. Together, the data suggest zipping,

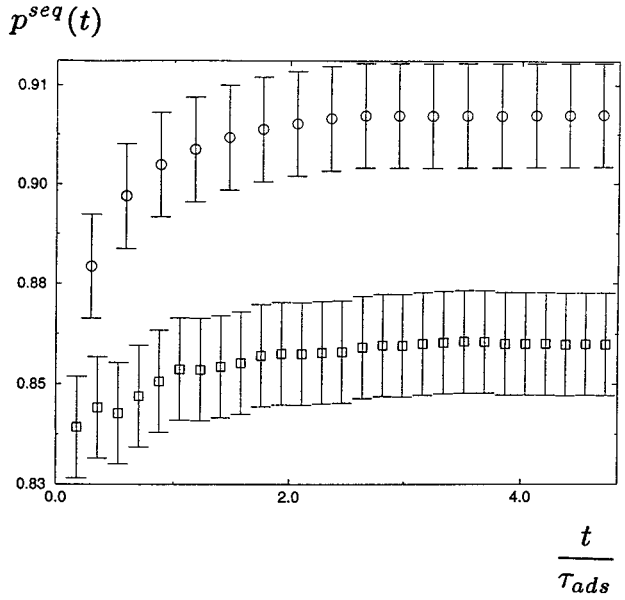

Figure 3. $p^{seq}(t)$ vs t/τ_{ads} for SAWs with $T_s = 0$, $N = 100$, $\zeta_s/\zeta_b = 1.0$, and two values of T_b: (○) $T_b \to \infty$; (□) $T_b = 0.25$. For averaging, $M \simeq 180$ and $\Delta t = 5 \times 10^3$ MCS.

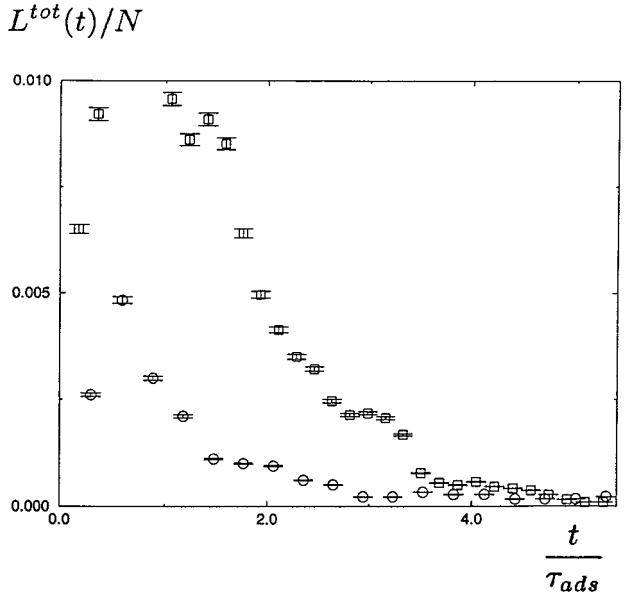

Figure 4. As in Figure 3, except that $L^{loop}(t)/N$ vs t/τ_{ads} is shown.

where the chain adsorbs predominantly by the sequential, consecutive attachment of monomers, a process that quickly erases loops established initially without creating new ones.

For fast adsorption, we found that τ_{ads} increases algebraically with chain length; i.e., $\tau_{ads} \sim N^{\alpha}$, $\alpha > 0$. For example, for SAWs with $T_s = 0$, $T_b \to \infty$, and $\zeta_s/\zeta_b = 1.0$, we found $\alpha = 1.57 \pm .07$, in agreement with Shaffer;[18] the results for a variety of other cases where $\tau_b/\tau_R \ll 1$ appear in Table 2. As mentioned, we found identical N-scaling for τ_{com} (Table 3), another measure of the time scale for adsorption based on the relaxation of the z component of $\mathbf{R}_{com}$. (The τ_{com} were determined from slopes of plots of log $\langle (R_g^2(t \to \infty) - R_g^2(t))\rangle / \langle (R_g^2(t \to \infty) - R_g^2(t=0))\rangle$ vs t.)

In every case where $\tau_b/\tau_R \ll 1$, we found that τ_{ads} falls considerably below the Rouse time, τ_R, indicating that adsorption forces long chains *strongly* out of equilibrium

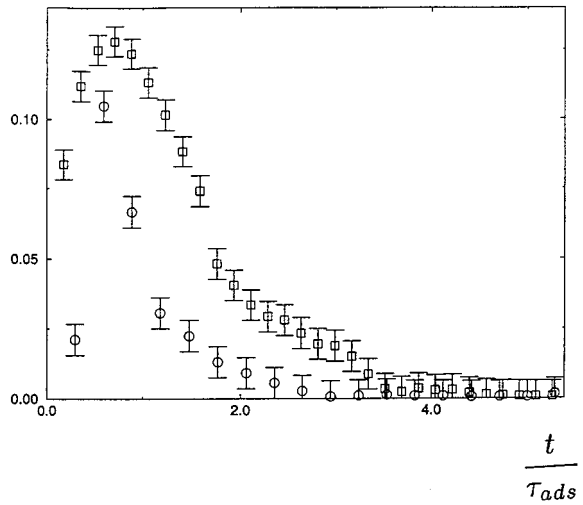

Figure 5. As in Figure 3, except that $N^{loop}(t)/N$ vs t/τ_{ads} is shown.

Table 2. Scaling Exponents α for *N*-Dependence of τ_{ads} for $T_s = 0$

T_b; ζ_s/ζ_b	SAW[a]	RW[b]
	$\tau_b/\tau_R \ll 1$	
$T_b \to \infty$; $\zeta_s/\zeta_b = 1.0$	1.57 ± 0.07	1.40 ± 0.09
$T_b \to \infty$; $\zeta_s/\zeta_b = 10.0$	1.74 ± 0.05	1.37 ± 0.07
$T_b \to \infty$; $\zeta_s/\zeta_b = 0.1$	1.54 ± 0.06	1.43 ± 0.08
	$\tau_b/\tau_R \lesssim 1$	
$T_b = 0.25$; $\zeta_s/\zeta_b = 1.0$	1.0 ± 0.1	0.94 ± 0.07
	$\tau_b/\tau_R > 1$	
$T_b = 0.1$; $\zeta_s/\zeta_b = 1.0$	0.8 ± 0.2	

[a] Self-avoiding-walk chain. [b] Random-walk chain.

Table 3. Scaling Exponents for *N*-Dependence of τ_{com} for $T_s = 0$

T_b; ζ_s/ζ_b	SAW[a]	RW[b]
	$\tau_b/\tau_R \ll 1$	
$T_b \to \infty$; $\zeta_s/\zeta_b = 1.0$	1.66 ± 0.07	1.4 ± 0.1
	$\tau_b/\tau_R \lesssim 1$	
$T_b = 0.25$; $\zeta_s/\zeta_b = 1.0$	0.9 ± 0.1	0.9 ± 0.1

[a] Self-avoiding-walk chain. [b] Random-walk chain.

in these cases. In other words, a deep energetic well with no local activation barrier sucks the chain onto the surface much faster than its Brownian motion would otherwise deliver it.

Note from Table 2 that, for the SAWs, α is independent of ζ_s/ζ_b for values $\lesssim 1$ but becomes marginally larger for $\zeta_s/\zeta_b = 10$, indicating a very weak effect of spreading kinetics on adsorption and flattening, in essential agreement with the deductions discussed earlier in connection with Figure 2. Interestingly, the α values for RWs all lie measurably *below* those for SAWs and are clearly *independent* of the surface friction. That the surface friction does not affect α *at all* for RWs makes sense, since there is no tendency to spread in this case; the equilibrium, in-plane size of a RW matches its initial footprint.[21]

D. Slow Adsorption ($\tau_b/\tau_R \gg 1$). Consider now cases resembling chemisorption. Here, a segment encounters a local barrier near the surface that blocks passage until fluctuations permit. When the characteristic time for passage of a segment to the surface τ_b exceeds the Rouse time, τ_R, the unadsorbed part of the chain is always relaxed, and every unattached segment visits the region near the interface many times. We find adsorption

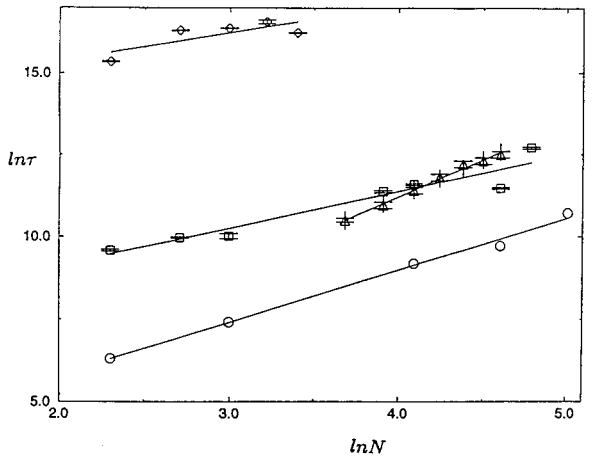

Figure 6. Ln τ_{ads} vs ln N for SAWs adsorbing onto a surface with a deep energy well ($T_s = 0$): (○) $T_b \to \infty$; (□) $T_b = 0.25$; (◇) $T_b = 0.1$. Shown also is the Rouse time τ_R for $D = 3$ (△).

dynamics very different from the case just discussed, where monomers adsorb as soon as they arrive at the interface, and the unattached part of the chain is driven out of equilibrium.

Simulating this case proved difficult because of the very long equilibration times. Consequently, preparing even a moderate number of samples for averaging could only be done with barriers giving $\tau_b/\tau_R \simeq 1$ at the highest N ($\sim 10^2$). In particular, we were able to simulate SAWs with a value of $T_b = 0.1$ ($\epsilon_b = 10kT$), corresponding to $\tau_b/\tau_R \simeq 1$ for $N = 100$. Of course, for $N < 100$, τ_b/τ_R lies considerably above unity in this case; for example, at $N = 10$, $\tau_b/\tau_R \simeq 100$. Because of the marginal statistics resulting with the $10kT$ barrier, we also performed calculations for a lower barrier height, $T_b = 0.25$ ($\epsilon_b = 4kT$), corresponding to $\tau_b/\tau_R \lesssim 1$, e.g., for $N = 10$, $\tau_b/\tau_R \simeq 10^{-1}$ and for $N = 100$, $\tau_b/\tau_R \simeq 10^{-3}$. These crossover data help to discern trends in behavior as τ_b/τ_R is increased toward the asymptotic limit $\tau_b/\tau_R \gg 1$. In all calculations involving a barrier, we fixed $T_s = 0$ and $\zeta_s/\zeta_b = 1.0$.

Even with a moderate barrier, $T_b = 0.25$ or $\epsilon_b = 4kT$, a dramatic mechanistic change occurs. Figures 3−5 show representative evidence with results for $N = 100$, $T_s = 0$. A local barrier of just $4kT$ significantly suppresses the sequential adsorption probability (Figure 3). At the same time, the barrier encourages formation of loops during adsorption, as shown in Figures 4 and 5, where the barrier causes the appearance of distinct peaks in the time history of the average number and size of loops. Evidently, even a modest local barrier discourages the tendency for zipping and switches on a new mechanism involving loop formation.

The N scaling of τ_{ads} with a local barrier was determined for both SAWs and RWs. Figure 6 shows log−log plots of τ_{ads} vs N for SAWs, and Table 2 collects all the values of α determined. Note from Figure 6 that even for the moderate barrier, $T_b = 0.25$, τ_{ads} still lies (marginally) above τ_R, whereas $\tau_R \gg \tau_{ads}$ without the barrier. Interestingly, the α values with a barrier all lie significantly *below* those for strong physisorption, where zipping dominates (Table 2), being about 1.0 for the moderate barrier, and smaller still for the high barrier, about 0.8. The α values for SAWs and RWs agree within the uncertainty.

Although the modest barrier of $4kT$ permitted very good sampling, giving reasonably low relative errors in the α, it clearly does not correspond to the asymptotic situation of interest ($\tau_b/\tau_R \gg 1$); rather, it corresponds to a crossover region. The calculations clearly in the asymptotic limit, using a much higher barrier, of $10kT$ ($T_b = 0.1$), succeeded to the extent that α was calculated with relative errors near ±25%. We can say for certain that in the limit $\tau_b/\tau_R \gg 1$ the exponent α lies *below* 1, in the range $0.6 < \alpha < 1.0$ for SAWs.

It is important to realize for the cases involving barriers that the adsorption time τ_{ads} *does not* fall significantly below the Rouse time even though α falls below the exponent for τ_R, namely, $1 + 2\nu_3$. The finding $\tau_{ads} \sim N^{\alpha}$ with $\alpha < 1 + 2\nu_3$ means that in the limit of infinitely long chains with a finite barrier height τ_{ads} eventually falls below τ_R. We believe that, in this limit, the system would return to a (coarse-grained) zipping process with α tending to about 1.6.

IV. Scaling Analysis

One can rationalize the exponents α obtained numerically with the help of a force balance on the adsorbing chain. Consider that during adsorption the surface exerts a mean suction force $F_{suction}$ on the chain in the $-z$ direction, which is resisted by a hydrodynamic, frictional drag $F_{friction}$ on the unadsorbed part moving through the bulk toward the surface; one can therefore write

$$F_{suction} + F_{friction} = 0 \tag{9}$$

Because of the short-ranged nature of the segment−surface interaction potential, the $F_{suction}$ acts only through monomers at "contact" points, i.e., at junctions between loops or tails and trains (Figure 1). Consequently, we assume

$$F_{suction} = N_c(t) f_c \tag{10}$$

where $N_c(t)$ is the instantaneous average number of contact points and f_c is the force per contact, presumed constant and independent of N. The hydrodynamic drag has the form

$$F_{friction} = \zeta_{tot}(t)\, \dot{R}_{com,z}(t) \tag{11}$$

where $\dot{R}_{com,z}(t)$ is the instantaneous average speed of the chain's center of mass toward the surface during adsorption, while $\zeta_{tot}(t)$ is the effective total friction coefficient on the unadsorbed part. Equations 9−11 are sufficient for a scaling-level estimate of α.

For this we replace $N_c(t)$ in eq 10 with an average over the time for adsorption, $\bar{N}_c$. Then, order-of-magnitude estimates of the terms in eq 11 are

$$\zeta_{tot}(t) \simeq \zeta_b \frac{N}{\bar{N}_c}; \quad \dot{R}_{com,z}(t) \simeq \frac{1}{\tau_{ads}} a \left(\frac{N}{\bar{N}_c}\right)^{\nu_3} \tag{12}$$

where a is the segment size. The first part of eq 12 estimates the friction coefficient to be that for an averaged size loop, while the second of eq 12 estimates the adsorption speed from the dimension of an average size loop and τ_{ads}. With eq 12, finding α from eqs 9−11 requires knowing how $\bar{N}_c$ scales with N, that is, knowing how the average number of loops developed during adsorption depends on the chain length.

Consider first the situation where monomers adsorb rapidly, $\tau_b/\tau_R \ll 1$. This occurs for long chains when there is no local activation barrier and corresponds roughly

to strong physisorption. We know from the simulations of this case that adsorption occurs rapidly, i.e., $\tau_b < \tau_{ads} \ll \tau_R$ (eq 8 and Figure 6), by a zipping mechanism where the number of contact points or loops remains approximately ~1 throughout, i.e.,

$$\bar{N}_c \sim N^0 \tag{13}$$

Eqs 9−11 then give

$$\tau_{ads} \sim N^{1+\nu_3}$$

i.e., $\alpha = 1.6$ for SAWs and $\alpha = 1.5$ for RWs, in excellent agreement with the results for RWs and SAWs from simulations (Table 2).

With a local barrier high enough that $\tau_b/\tau_R \gg 1$, we know from simulations that $\tau_{ads} > \tau_b \gg \tau_R$ (eq 8 and Figure 6). This corresponds to chemisorption. Here, the chain stays tethered to the interface, and in virtual equilibrium during adsorption. Each monomer visits the barrier many times by $t \sim \tau_{ads}$, and a fraction succeeds in penetrating to the surface, forming contact points and loops. In principle, the number of monomers that traverse the barrier and form contacts in time τ_{ads} is proportional to the total number of collisions monomers make with the surface. The simplest hypothesis is that all unadsorbed segments visit the barrier with the same frequency, of order $\bar{\tau}_R^{-1}$, where $\bar{\tau}_R$ is the Rouse time for an average sized loop, so that the total number of collisions is of order $N\tau_{ads}/\bar{\tau}_R$ and therefore

$$\bar{N}_c \sim N\frac{\tau_{ads}}{\bar{\tau}_R}$$

This gives

$$\tau_{ads} \sim N^{2\nu_3/2-\nu_3}$$

or $\alpha = {}^6/_7$ for SAWs and $\alpha = {}^2/_3$ for RWs. Both of these estimates lie near the value $\alpha = 0.8 \pm 0.2$ found by simulations of SAWs with the higher barrier of $10kT$ (Table 2) and just below those for the crossover case with a moderate barrier of $4kT$ where $\tau_{ads} \simeq \tau_R > \tau_b$ (Figure 6).

V. Summary and Conclusions

We studied adsorption kinetics of an isolated polymer in two limiting situations corresponding roughly to strong physisorption and chemisorption. This was accomplished by a coarse-grained lattice simulation including a strong, short-ranged attractive potential between the segments and the surface. Strong physisorption was mimicked by including a deep energy well at the surface in the segment−surface interaction, while chemisorption also included a local activation barrier separating the surface well from the bulk. These situations correspond to drastically different values of the characteristic ratio τ_b/τ_R, where τ_b refers to the passage time for a segment near the surface through the barrier and τ_R means the bulk Rouse time. Physisorption corresponds to small values of this ratio, while chemisorption is the opposite limit. We found qualitatively different adsorption processes in the two cases. Extra surface friction was included in the model, but it did not affect the salient aspects of the adsorption kinetics in either case.

The case corresponding to strong physisorption yields fast adsorption with a characteristic time τ_{ads} well below the chain's relaxation time. The process occurs by "zipping", a sequential adsorption of monomers, which quickly erases loops and forces the chain strongly out of equilibrium. The N-scaling of τ_{ads}, $\tau_{ads} \sim N^{1.58}$, can be explained by a simple force balance, including external forces on segments near the interface arising from interactions with the wall. These show up via the instantaneous average number of contact points the chain makes with the surface. Zipping corresponds to maintaining the initial number of contacts (i.e., loops) throughout adsorption, with monomers adsorbing sequentially according to how close they are from the nearest contact point.

The adsorption kinetics are dramatically different when a local activation barrier is imposed, as in chemisorption or grafting. If the barrier is high enough to ensure $\tau_b/\tau_R > 1$, zipping is quenched and loop formation occurs during deposition; monomers remote from the surface are as likely to attach as those near to it. The characteristic time τ_{ads} now lies considerably above τ_R and has a different N-scaling. The result can be explained with the same force balance, assuming that the average number of loops formed during adsorption increases with N. It should be noted that, for a fixed barrier height, this regime can only be accessed for finite N.

These calculations show that the global dynamics of the chain, i.e., the longest wavelength features and the corresponding time scales, are influenced dramatically by changes in local scale features, in particular the details of the segment−surface interaction potential. This is unusual in polymer systems.

Acknowledgment. The authors acknowledge helpful discussions with B. O'Shaughnessy (Columbia) and N. Turro (Columbia) and financial support from the National Science Foundation (Grant CTS-96-34594) and the U.S. Department of Energy (LDRD/CD on Science of Polymer Aging).

VII. Appendix A

The sequential adsorption probability, $p^{seq}(t)$, does not fall to zero in the complete absence of zipping. Consequently, to judge when zipping occurs on the basis of $p^{seq}(t)$, one has to compare measured values to an appropriate benchmark. Consider the case where one ignores spatial correlations among monomers, i.e., the probability that monomer n adsorbs does not depend on the location of other monomers. For an infinitely deep surface well ($T_s = 0$), once a segment adsorbs it cannot desorb, so that

$$p^{seq}(t \to \infty) = \frac{\int_0^N \mathrm{d}n\, p(n)}{N} \tag{14}$$

where n is an index for the adsorption events and $p(n)$ is the probability that the adsorption n adsorbs with either monomer $n - 1$ or $n + 1$ or both already on the surface, under the condition that $n - 1$ monomers are already adsorbed. This can be expressed as

$$p(n) = \frac{2C_{N-3}^{n-1} + C_{N-3}^{n-2}}{C_{N-1}^{n}}; \quad C_N^n = \frac{N!}{n!(N-n)!} \tag{15}$$

since $p(n)$ is equal to the ratio of the number of ways for monomer n to have a "right" neighbor plus the number of ways for it to have a "left" neighbor plus the number of ways for it to have two neighbors, regardless of order; to the number of ways for n monomers out of N to be on the surface, regardless of order.

After the integration in eq 14 one obtains

$$p^{\mathrm{seq}}(t \to \infty) = \frac{N(^2/_3 N - {}^3/_2)}{(N-1)(N-2)} \tag{16}$$

which has the large N limit of $^2/_3$, an appropriate benchmark.

References and Notes

(1) Fleer, G. J.; Cohen Stuart, M. A.; Scheutjenns, J. M. H. M.; Cosgrove, T.; Vincent, B. *Polymers at Interfaces*; Chapman Hall: London, 1993.

(2) Balazs, A. C. *MRS Bull.* **1997**, *22* (January).

(3) Grest, G. S.; Murat, M. *Monte Carlo and Molecular Dynamics Simulations in Polymer Science*; Binder, K., Ed.; Oxford: New York, 1995; Chapter 5.

(4) Tirrell, M.; Levicky, R. *Curr. Opin. Solid State Mater. Sci.* **1997**, *2*, 668.

(5) Barford, W.; Ball, R. C. *J. Chem. Soc., Faraday Trans 1* **1987**, *83*, 2515.

(6) Chakraborty, A. K.; Shaffer, J. S.; Adriani, P. M. *Macromolecules* **1991**, *24*, 5226.

(7) Konstadinidis, K.; Prager, S.; Tirrell, M. *J. Chem. Phys.* **1992**, *97*, 7777.

(8) Schneider, H. M.; Frantz, P.; Granick, S. *Langmuir* **1996**, *12*, 994.

(9) King, S. M.; Cosgrove, T. *Macromolecules* **1993**, *26*, 5414.

(10) Schwartz, D. C.; Samad, A. *Curr. Opin. Biotechnol.* **1997**, *8*, 70.

(11) Wang, W. N.; Lin, J. Y.; Schwartz, D. C. *Biophys. J.* **1998**, *75*, 513.

(12) Carmesin, I.; Kremer, K. *Macromolecules* **1989**, *21*, 2819.

(13) Wittmann, H. P.; Kremer, K. *Comput. Phys. Commun.* **1990**, *61*, 309. Wittmann, H. P. *Comput. Phys. Commun.* **1992**, *71*, 343. Paul, W.; Binder, K.; Heermann, D. W.; Kremer, K. *J. Phys. II* **1991**, *1*, 37. Paul, W.; Binder, K.; Heermann, D. W.; Kremer, K. *J. Chem. Phys.* **1991**, *95*, 7726.

(14) Deutsch, H. P.; Binder, K. *J. Chem. Phys.* **1991**, *94*, 2294.

(15) Lai, P. Y. *Phys. Rev. E* **1994**, *49*, 5420.

(16) Lai, P. Y. *Macromol. Theory Simul.* **1996**, *5*, 255.

(17) Eisenriegler, E.; Kremer, K.; Binder, K. *J. Chem. Phys.* **1982**, *77*, 6296.

(18) Shaffer, J. S. *Macromolecules* **1994**, *27*, 2987.

(19) Metropolis, N.; Rosenbluth, A. W.; Rosenbluth, M. N.; Teller, A. H.; Teller, E. *J. Chem. Phys.* **1953**, *21*, 1087.

(20) Binder, K.; Heerman, D. W. *Monte Carlo Methods in Statistical Physics: An Introduction*; Springer-Verlag: New York, 1988; pp 17−35.

(21) de Gennes, P. G. *Scaling Concepts in Polymer Physics*; Cornell University Press: Ithaca, NY, 1979.

(22) Doi, M.; Edwards, S. F. *The Theory of Polymer Dynamics*; Oxford: New York, 1986.

(23) Ponomarev, A. L.; Sewell, T. D.; Durning, C. J. *J. Polym. Sci. Part B: Polym. Phys.*, in press.

(24) Binder, K. *Monte Carlo and Molecular Dynamics Simulations in Polymer Science*; Binder, K., Ed.; Oxford: New York, 1995; Chapter 7.

MA9808732